Astron. Astrophys. 269, 67–76 (1993)

ASTRONOMY AND ASTROPHYSICS

The proton blazar

K. Mannheim

Max-Planck-Institut für Radioastronomie, Auf dem Hügel 69, W-5300 Bonn 1, Germany

Received July 8, accepted September 8, 1992

Abstract. Recent gamma ray detections and the radio/X-ray correlation of extragalactic flat-spectrum radio sources make the existence of an ultra–relativistic proton population in jets very probable. The protons with maximum Lorentzfactors in the range $10^9 - 10^{11}$ generate hard photons with energies from keV to TeV via pion and pair photoproduction and subsequent synchrotron cascade reprocessing.

In this paper relativistic protons are considered in the context of the Blandford & Königl (1979) model of compact radio jets which are assumed to be responsible for the nonthermal emission component of flat–spectrum quasars and BL Lacertids. The baryons are simply added to the electrons considered as the only radiative agent in the original work.

The differential gamma ray spectrum induced by the protons is an inverse power–law with an index preferentially in the range 1.8 to 2.0. Below a few MeV the spectrum flattens to an X–ray spectrum with index 1.5 to 1.7. For a given energy flux through a jet the apparent radio luminosity is lower for a relativistic proton enriched plasma than for a relativistic electron enriched plasma (*i.e.* for jets with a proton/electron energy density ratio $\eta = u_p/u_e > 1$), while the apparent gamma ray luminosity is almost constant.

Differential Doppler–boosting, *i.e.* changes in flux amplification due to changes in the orientation of the radiating plasma element, influences the pair creation optical depth and therefore has an effect on the maximum photon energies of the compact radio source. Hence TeV emission should correlate with high states of the entire continuum flux.

Further consequences are a) an observable diffuse flux of neutrinos with a flat spectrum in the PeV–EeV range, b) a diffuse flux of gamma rays equal to the flux of gamma rays from the Milky Way at an energy of 7 TeV, c) neutrons escaping the blazar that convert their luminosity in the kinetic power of a conical wind surrounding the jet or escape the host galaxy at highest energies.

Key words: Elementary particles – BL Lacertae objects: general – Galaxies: jets – Gamma rays: theory – X–rays: galaxies

Send offprint requests to: K. Mannheim

1. Introduction

Extragalactic radio sources are the largest known dissipative structures (nonthermal objects) known in the universe and as such highly interesting candidate sources of cosmic rays (see references in Berezinskiĭ et al. 1990). There are two ways for them to inject cosmic ray baryons into the intergalactic medium; (i) by escape from hot spots often a few hundred kiloparsecs away from active nucleus of the host galaxy (Biermann 1991; Rachen & Biermann 1992) and (ii) by neutron escape from the sub–parsec scale of the jet or the nucleus (Protheroe & Szabo 1992). Both these mechanisms avoid adiabatic losses preventing such escape otherwise. Do we have any indications that baryons are actually present in radio jets?

The leptonic component ($e^{\pm}$) of nonthermal particles in jets are the well–studied origin of synchrotron radiation from radio to X-ray frequencies (e.g. see the conference proceedings edited by Maraschi et al. 1989; Zensus et al. 1987; Bregman 1990). Subtracting thermal emission components like dust infrared radiation and the big blue bump in quasars one is left with a continuum spectrum of highly varying flux and polarization. Flat–spectrum radio sources are characterized by jets oriented at small angles to the line of sight, so that the radiation from the base of the jet is Doppler–boosted towards the observer. Some of these sources, the blazars, show very active behaviour of the most compact regions of the jet, especially with respect to polarization. Probably all flat–spectrum radio sources appear as blazars during active episodes. To simplify things the compact jet with relativistic electrons and protons shall be coined the "proton blazar" throughout this work.

Since the fact that particle acceleration takes place in radio jets is obvious from synchrotron observations, it is a small speculative step to argue that this acceleration mechanism not only concerns electrons (and positrons), but protons (and nuclei) as well. However, the step is really not speculative, because it has already been shown that in principle the gamma radiation from flat–spectrum radio sources detected by GRO can be explained as proton initiated synchrotron cascade emission in radio jets (Mannheim & Biermann 1992) assuming that protons are shock accelerated up to energies of 10^{11} GeV. The cascade emission ranges from X-rays to gamma rays competing with synchrotron–self–Compton (SSC) emission (Königl

1981). The cascade spectrum is always harder than $\alpha_X = 1$, so that the luminosity of this mechanism peaks in the gamma ray band, unless there is thermal reprocessing (Zdziarski et al. 1990). This raises the question of how far one can actually interpret nonthermal emission above keV as proton induced and what properties determine the high energy blazar spectrum. The physical conditions inferred may – among other things – help to elucidate the role of extragalactic jets as sources of cosmic rays.

To this end one must specify the proton and electron distributions in a physically constrained plasma volume element. The Blandford & Königl (1979) model of compact relativistic jets shall serve as a conceptual guideline here (BK model hereafter). Models of shock acceleration explain how particle acceleration in jets possibly works (e.g. Ellison et al. 1990). One important cooling channel of the protons is photomeson (mainly pion) production (Sikora et al. 1987). The pions decay yielding neutrinos, pairs and gamma rays. Both, the weak and the electromagnetic fraction of the pion power, have very important observational consequences.

Neutrino detection is feasible with experimental designs currently under construction like AMANDA, DUMAND II or BAIKAL (Stenger et al. 1992) in the TeV range, by advanced analysis of horizontal atmospheric showers up to the PeV range (Halzen & Zas 1992) and at still higher energies with the High Resolution Fly's Eye (Cassiday et al. 1989). Extragalactic neutrino beams would be a unique tool for elementary particle physics to study weak interactions in a kinematical regime far beyond planned laboratory designs.

In contrast to the neutrinos the electromagnetic power injected into the compact jet at energies far above TeV is observable only through the action of several reprocessing cycles with pair creation followed by synchrotron radiation. The target photons are again, self–consistently as for the protons, the soft synchrotron photons from the primary electrons. Such electromagnetic showers redistribute the power down below the critical energy E_γ^* where the compact jet is optically thick to pair creation (Burns & Lovelace 1982; Svensson 1987; Berezinskiĭ et al. 1990, and references therein). In the BK model it turns out that the typical energy (as seen in the observer's frame) is in the TeV range. The showers are therefore unsaturated in the sense that not all photons with sufficient energy to create a pair (with energy above twice the electron rest mass) do actually create a pair. As a consequence a detectable annihilation line does not form.

The critical energy is commonly expressed in terms of the radiation compactness l, which is proportional to the energy–dependent pair creation optical depth $\tau_{\gamma\gamma}(E_\gamma) \simeq 0.1 l E_\gamma / m_e c^2$ at electron rest mass energy. Assuming isotropic emission in the comoving frame of a relativistic jet the target radiation compactness is given by

$$l \simeq \frac{\sigma_T}{4\pi m_e c^3}\frac{L_s}{r'} \simeq 2.1\times 10^{-30}\frac{L_s \sin\theta}{r_{ob}\gamma_j} \simeq 10^{-5} \times \left[\frac{L_s}{10^{43}\,\mathrm{erg/s}}\right]\left[\frac{\gamma_j}{10}\right]^{-1}\left[\frac{r_{ob}}{10^{-2}\,\mathrm{pc}}\right]^{-1}\frac{\sin[\theta]}{\sin[10^o]} \quad (1)$$

where the comoving frame synchrotron luminosity is given by

$$L_s = D_j^{-p} L_{(obs)} \quad (2)$$

with $p = 4$ (Urry & Shafer 1984), the observed source luminosity is $L_{(obs)}$ and the Lorentzfactor, speed of the jet and angle to the line of sight are γ_j, β_j and θ, respectively. Here

$$D_j = \left[\gamma_j(1-\beta_j\cos\theta)\right]^{-1} \quad (3)$$

denotes the Doppler–factor of the jet which can be estimated from superluminal expansion of VLBI knots yielding near maximum flux amplification $D_j \approx \gamma_j \approx 2-10$, so that $L_s \ll L_{(obs)}$. The length r of the conical jet projected on the line of sight is given by $r_{ob} = r\sin\theta$ and the intersection of the l.o.s. with the jet in the comoving frame is given by $r' = r_{ob}\gamma_j/\sin\theta$ provided the bright part of the jet is viewed along its entire length.

From Eq. (1) one obtains for a target spectral index $\alpha = 1$ the critical energy in the observer's frame

$$E_\gamma^* \simeq 10 D_j l^{-1}\,\mathrm{MeV} \simeq 10\,\mathrm{TeV} \times \left[\frac{L_s}{10^{43}\,\mathrm{erg/s}}\right]^{-1}\left[\frac{r_{ob}}{10^{-2}\,\mathrm{pc}}\right]\left[\frac{\gamma_j D_j}{100}\right]\left[\frac{\sin[\theta]}{\sin[10^o]}\right]^{-1} \quad (4)$$

Thus gamma rays even up to 10 TeV can be emitted by blazars in detailed accordance with recent GRO (Hartman et al. 1992) and Whipple (Punch et al. 1992) observations. The fact that $L_s \ll L_{(obs)}$ is actually a nice property in the framework of unifying models, where flat–spectrum radio quasars are assumed to be Fanaroff–Riley class II (FR II) galaxies (Fanaroff & Riley 1974) with the jet viewed at small angles to the line of sight. In this case the radiative dissipation in the nuclear jet must be only marginal – otherwise the core would not be able to sustain the large–scale jet of the radio galaxy with its enormous kinetic luminosity. The kinetic luminosity of the jet must exceed the synchrotron luminosity $L_s \approx 10^{44}$ erg/s of hot spots at the ends of FR II galaxies.

The organization of the paper is as follows: Firstly, properties of a typical synchrotron component in the BK model are described including relativistic electrons and protons. Results are then compared to observed properties of 3C279 and Mkn421. Hereby I demonstrate the action of parameters involved with the model. Secondly, an estimate of the gamma ray and neutrino background contribution from proton blazars is obtained. Finally, the consequences of biconical escape of neutrons are studied.

2. A rudimentary proton blazar model and its consequences

In this section I refer to the explanation of flat–spectrum radio sources as compact relativistic jets demonstrated in the model of Blandford & Königl (1979) by simply *adding* a population of accelerated protons. The protons cool in the synchrotron photon atmosphere generated by the accelerated electrons.

The striking discovery of intraday radio variability emphasizes the fact that shocks in compact jets may indeed be the accelerating agent of blazars (Witzel 1990). As a matter of fact, the

extremely short time scale of the variations can be explained best by relativistic shocks propagating down a relativistic bulk flow with embedded inhomogenities (Qian et al. 1990). When the trajectories of the shocks are not linear, but helical as suggested by VLBI pictures or when the distribution of inhomogenities is ordered, the resulting variability pattern may even be quasi–periodic as observed in 0716+714 (Quirrenbach et al. 1991). The BK compact jet may therefore be considered a crude approximation to the downstream regions of multiple, probably oblique and relativistic shocks propagating through a jet flow coming out of an AGN.

2.1. The model

In the Blandford and Königl model it is assumed that electrons are accelerated in a supersonic conical jet of opening angle Φ yielding a synchrotron spectrum locally with the optical thin index $\alpha = 0.5$ up to the break frequency determined by equal loss and expansion time scales, respectively, *viz.*

$$t_e = 7.7 \times 10^8 \gamma_j B^{-2} \gamma_e^{-1} \text{ s} \tag{5}$$

and

$$t_{exp} = 10^8 r_{ob} (\sin\theta)^{-1} \beta_j^{-1} \text{ s} \tag{6}$$

where $B = B_1 (r/1\,\text{pc})^{-1}$ denotes the magnetic field strength in the jet (in Gauss). Above the break frequency (in the observer's frame and in units of GHz) $\nu_{b9} = 4.2 \times 10^{-3} (1+z)^{-1} D_j B \gamma_{e,b}^2$ the spectrum is loss dominated, so that $\alpha = 1$ up to the maximum frequency determined by equal acceleration and loss time scale (Biermann & Strittmatter 1987) provided the acceleration time scale remains shorter than the expansion time at the maximum energy. Corresponding particle distributions break from $dN/dE \propto E^{-2}$ to $dN/dE \propto E^{-3}$. The dimensionless break energy of the electron distribution is given by

$$\gamma_{e,b} = 7.7 \gamma_j \beta_j B_1^{-2} r_{ob} (\sin\theta)^{-1} \tag{7}$$

Inserting the magnetic field strength

$$B_1 = 0.04 \Delta^{-\frac{1}{2}} \left(1 + \frac{2}{3} k_e \Lambda_e\right)^{-\frac{1}{2}} \gamma_j^{-1} \beta_j^{-\frac{1}{2}} (\sin\theta)^{-1} \Phi_{ob}^{-1} L_{44}^{\frac{1}{2}} \tag{8}$$

at the radius $r_{b,ob}$ (in parsec) where the maximum brightness temperature is achieved

$$r_{b,ob} = 0.04 k_e^{\frac{1}{6}} \Delta^{-\frac{13}{12}} \left(1 + \frac{2}{3} k_e \Lambda_e\right)^{-\frac{13}{12}} \gamma_j^{-\frac{19}{6}} \beta_j^{-\frac{25}{12}} D_j^{-\frac{1}{6}} \times (\sin\theta)^{-\frac{7}{6}} \Phi_{ob}^{-2} L_{44}^{\frac{13}{12}} \tag{9}$$

yields the electron break energy

$$\gamma_{e,b} = 200 k_e^{\frac{1}{6}} \Delta^{-\frac{1}{12}} \left(1 + \frac{2}{3} k_e \Lambda_e\right)^{-\frac{1}{12}} \gamma_j^{-\frac{1}{6}} \beta_j^{-\frac{1}{12}} D_j^{-\frac{1}{6}} \times (\sin\theta)^{-\frac{1}{6}} L_{44}^{\frac{1}{12}} \tag{10}$$

Here the notation is the same as in Blandford & Königl (1979), *i.e.* $\Phi_{ob} = \Phi/\sin\theta$, L_{44} denotes the luminosity of the jet due to the energy flux in relativistic particles and fields in units of 10^{44} erg/s, $\Delta = \ln r_{max}/r_{min} \approx 5$, $\Lambda_e = \ln \gamma_{e,max}/\gamma_{e,min} \approx 4$. One important consequence of including protons is, however, that k_e^{BK} defined by $k_e^{BK} \Lambda_e = u_e/u_B$ where u denotes energy density has to be replaced by

$$k_e = k_e^{BK} (1+\eta)^{-1} \tag{11}$$

where the energy density ratio of protons and electrons is given by

$$\eta = \frac{u_p \Lambda_p}{u_e \Lambda_e} \tag{12}$$

In order to obtain the break energy of the proton distribution one must equal the expansion time scale with the energy loss time scale for protons. The ratio of electron and proton cooling time scales is given by

$$\frac{t_p(\gamma_e)}{t_e(\gamma_p)} = \left[\frac{m_p}{m_e}\right]^3 \left[\frac{\gamma_e}{\gamma_p}\right] \left[\frac{1+a_s}{1+240 a_s}\right] \tag{13}$$

where the ratio of energy in synchrotron photons to the magnetic field is denoted

$$a_s = \frac{u_s}{u_B} \approx k_e \beta_j \gamma_j \Phi \tag{14}$$

The electron cooling time scale involves synchrotron and first–order self–Compton emission, the proton cooling time scale involves synchrotron and pion production losses. The Bethe–Heitler pair luminosity is less than 50% of the pion luminosity due to the low value $\langle \kappa\sigma \rangle_{e^\pm} \approx 1\ \mu$b peaking at proton rest frame photon energies of roughly $10 m_e c^2$ compared to $\langle \kappa\sigma \rangle_\pi \approx 50\ \mu$b at a threshold energy in the proton rest frame of $280 m_e c^2$. Additional suppression results from the fact that target photons close to the threshold energy are found at lower frequencies for pair production than for pion production. However, at lower frequencies the target spectrum is flat ($\alpha = 0$). Compared to proton synchrotron radiation with characteristic synchrotron photon energy $E_\gamma(\text{p, syn}) = 1.6 \times 10^{-17} B_\perp \gamma_p^2$ MeV pion production wins for values $a_s > 0.005$. Hence putting $t_{exp} = t_p$ one obtains

$$\gamma_{p,b} = \left[\frac{m_p}{m_e}\right]^3 \frac{1+a_s}{1+240 a_s} \gamma_{e,b} = 6 \times 10^9 \frac{1+a_s}{1+240 a_s} \gamma_{e,b} \tag{15}$$

and then

$$\frac{Lp}{L_e} \approx \frac{u_p}{u_e} \frac{t_e(\gamma_{e,b})}{t_p(\gamma_{p,b})} = \eta \tag{16}$$

Realizing that the proton induced luminosity dominates the hard X– and gamma ray range, whereas the electron induced luminosity dominates the radio to UV range, one obtains

$$L(>X)/L(<UV) \approx 1 \quad \text{for} \quad \eta = 1.$$

However, when the acceleration time scale equals the expansion time scale already at an energy $\gamma_p^* < \gamma_{p,b}$, the proton

distribution will be essentially cut off at γ_p^*. *E.g.*, the acceleration time scale for shock acceleration at nonrelativistic shocks in fully developed Kolmogorov turbulence given in Biermann & Strittmatter (1987) leads to this situation in compact jets. In this case the cooling time scales of protons and electrons are not the same at their maximum (resp. break) energies and hence the induced photon luminosities will only be comparable, if a greater proton/electron ratio compensates for the longer cooling time scale of the protons (Mannheim & Biermann 1992). Another problem related to the extremely high proton break energy Eq. (15) is that the model is close to the limits imposed by the geometry of the source (Bell 1978). The ratio of the radius of gyration of a proton $r_g = 10^{-12}B^{-1}\gamma_p$ at the break energy to the transverse size of the jet $r_\perp \approx r_{b,ob}\Phi_{ob}$ at the radius r_b of the maximum brightness temperature is given by

$$\frac{r_g(\gamma_{p,b})}{r_\perp(r_{b,ob})} = 30k_e^{\frac{1}{6}}\Delta^{\frac{5}{12}}\left(1+\frac{2}{3}k_e\Lambda_e\right)^{\frac{5}{12}}\gamma_j^{\frac{5}{6}}\beta_j^{\frac{5}{12}}D_j^{-\frac{1}{6}} \times (\sin\theta)^{-\frac{1}{6}}L_{44}^{-\frac{5}{12}}\frac{1+a_s}{1+240a_s} \quad (17)$$

Note that extremely high proton energies $E_p > 10^9$ GeV imply that the escaping flux of neutrons resulting from pion production on the photon target $p+\gamma \rightarrow n+\pi^+$ can escape the radio galaxy and contribute after β-decay to the flux of cosmic rays observed at earth (for cosmic rays of a neutron origin from radio–quiet AGN cf. Protheroe & Szabo 1992).

A further important parameter is the compactness of the relativistic jet. It is calculated from Eq. (1) yielding at the radius $r_{b,ob}$

$$l = 9\times10^{-4}k_e^{\frac{5}{6}}\Delta^{\frac{13}{12}}\left(1+\frac{2}{3}k_e\Lambda_e\right)^{\frac{1}{12}}\gamma_j^{\frac{13}{6}}\beta_j^{\frac{25}{12}}D_j^{\frac{1}{6}} \times (\sin\theta)^{\frac{13}{6}}\Phi_{ob}^2L_{44}^{-\frac{1}{12}} \quad (18)$$

Equations (4), (15) and (18) imply that the photons from pion decay with mean energy at the maximum of the emissivity $\langle E_\gamma\rangle \simeq 0.1E_{p,b}$ are fully reprocessed by a synchrotron casacade $\gamma+\gamma_s \rightarrow e^+ + e^-$, $e+\gamma^* \rightarrow e+\gamma$, $\gamma+\gamma_s \rightarrow e^+ + e^-$, etc. ($\gamma_s$ denotes a soft target photon and γ^* denotes a virtual transversal photon of the magnetic field), until the electromagnetic power finally shows up below the TeV range. The cascade is started only because the pion flux is flat, so that the injection of power has its maximum at the maximum pion energy[1]. The dominant target photons for pion production are the photons with $\nu > \nu_b$, since they only satisfy the threshold condition for pion production justifying the assumption $\alpha = 1$ for the target field (the target photons at threshold for pair production have $\nu \ll \nu_b$ reducing their contribution).

[1] A detailed description of the physics of the proton initiated cascade (PIC) is given in Mannheim et al. (1991), hereafter refered to as MKB. The reader may demonstrate him/herself the action of the reprocessing cycles by calculating back-of-the-envelope sequentially π^o decay photon injection, photon-photon pair production, synchrotron radiation, pair production etc. until the characteristic synchrotron frequency is below the value Eq. (4).

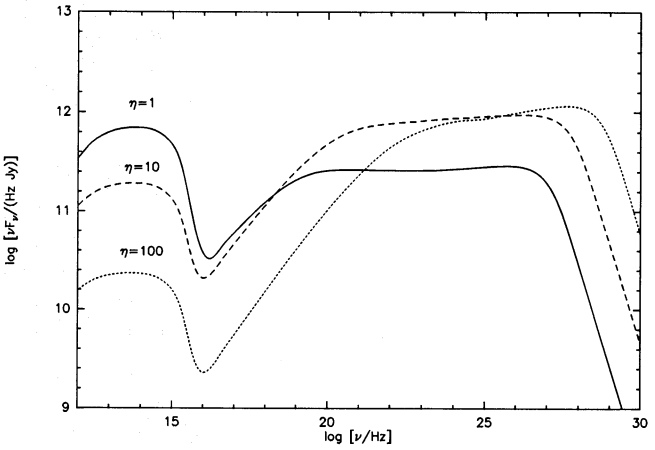

Fig. 1. The variation of the proton blazar spectrum with the proton/electron ratio η. Parameters are $\theta = 7^o$, $L_{44} = 1$, $z = 0.1$, $\Delta = 5$, $\Lambda_e = 4$, $\Lambda_p = 20$, $k_e^{BK} = 0.5$, $\gamma_j = 5$.

2.1.1. The relative contribution of secondaries from pp and pγ collisions, respectively

Since the energy loss time scale for pp collisions is constant, in contrast to the pγ losses described above, the emissivity of secondaries from pp collisions is much steeper, *i.e.* reflects the power law of the protons. This is especially important for the neutrino flux from proton blazars, which is flat for pγ collisions, but has a E^{-1} power–law for pp collisions. Therefore the neutrinos from pp collisions are important at lower neutrinos energies than the neutrinos from pγ collisions. In order to estimate the relative contributions one can readily calculate the ratio $L_\nu(pp)/L_\nu(p\gamma)$ of the neutrino luminosity (or photon luminosity analogously) induced by pp and pγ collisions, respectively.

The thermal gas density in jets is limited by the fact that the kinetic energy of the jet flow should remain less than or equal to the Eddington luminosity of the AGN producing the jet.

$$L_{kin} = An_{th}m_pc^3\gamma_j\beta_j \leq L_{edd} = 1.3\times10^{46}M_8\,\mathrm{erg\,s^{-1}} \quad (19)$$

where $A = 3.4\times10^{34}r^2$ cm^2 denotes the cross sectional area of the jet at length r (in parsec) for an intrinsic opening angle of $\Phi = 2^o$, $\gamma_j \simeq 10$ and M_8 denotes the mass of a central black hole in units of 10^8 solar masses $M_\odot$. From Eq. (19) one obtains

$$n_{th} \leq 7.9\times10^2M_8r^{-2}\,\mathrm{cm^{-3}} \quad (20)$$

Now the pp energy loss time scale is given by

$$t_{pp} = \left[n_{th}c\sigma_{pp}\right]^{-1} \quad (21)$$

with $\sigma_{pp} \simeq 3\times10^{-26}$ cm^2. From Eqs. (5), (7) and (21) it follows that

$$\frac{L_\nu(pp)}{L_\nu(p\gamma)} = \frac{t_{p\gamma}(\gamma_{p,b})}{t_{pp}} \leq 7\left[\frac{r_S}{r}\right] \quad (22)$$

where $r_S \simeq 10^{-5}M_8$ denotes the Schwarzschild radius. Thus even at the base of the jet, where $r \approx 10r_S$, photon cooling is the dominant source of secondaries.

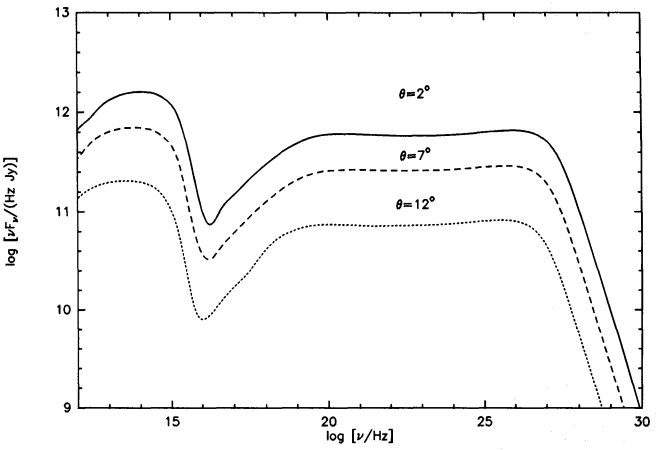

Fig. 2. The variation of the proton blazar spectrum with the angle to the line of sight θ. Parameters are as above with $\eta = 1$.

2.2. *The spectrum*

With the proton and electron distributions, as well as the magnetic field and the compactness specified by the model one can calculate the resulting PIC spectrum choosing a proper value of the proton/electron ratio. As a matter of fact, when gamma ray observations have been performed one can estimate the proton/electron ratio from $\eta = L(>X)/L(<UV)$, cf. Eq. (16). The target spectrum for the cascade is the integrated spectrum over the compact jet which has the global spectral index $\alpha = 0$ up to $\nu_{\rm b,ob}$ and then $\alpha = 1$ up to the maximum primary electron synchrotron frequency at $\nu_{\rm c} = 10^{14-16}$ Hz. Although the flatness of the radio spectrum follows from the Blandford and Königl model, the shock origin of the accelerated particle populations emphasizes the importance of a non–continuous distribution of surface brightness (separation of shocks) and hence to a smoother transition $\alpha = 0 \rightarrow \alpha = 1/2 \rightarrow \alpha = 1$ to the loss dominated spectrum. *I.e.*, strong individual shocks seemingly important in blazars where they cause the extremely rapid variability may show up with their optically thin index $\alpha = 1/2$ at frequencies just below $\nu_{\rm b,ob}$ (cf. Kellermann & Pauliny–Toth 1969).

The stationary spectrum of the PIC is obtained by solving the coupled transport equations of secondary pairs and photons in the high energy limit ($\nu_{\rm PIC} \gg \nu_{\rm c}$ where $\nu_{\rm c} \approx 10^{14-16}$ Hz refers to the characteristic synchrotron frequency of electrons at the maximum energy corresponding to equal acceleration and cooling time scales) as shown in MKB. In this limit the showers develop fully linear in the soft photon soup of the accelerated electrons, thereby redistributing the power injected at highest energies rather smoothly between hard X–rays and gamma rays up to 1–10 TeV. The shape of the spectrum results from merging of individual cascade generations tending to yield the spectral index $\alpha_\gamma = 1$ (equal power per decade of energy). The upper turnover is determined by E_γ^* from Eq. (4) and the break towards the X–ray spectrum with $\alpha_X = 0.5 - 0.7$ is determined by the characteristic synchrotron frequency of the pairs produced by gamma rays at E_γ^*, *i.e.* $E_\gamma^{**} \simeq 10^{-12} B_\perp D_{\rm j}^2 l^{-2}$ MeV. So $E_\gamma^{**} \simeq$ MeV for typical values $B_\perp = 1$ G, $D_{\rm j} = 10$ and $l = 10^{-5}$.

Since $a_{\rm s} < 1$ for a quasi–stationary synchrotron source and since the virtual photon scattering in the rest frame of the radiating electron is still nonrelativistic, the emission is optically thin (nonrelativistic) synchrotron radiation even at these high energies.

With given values of $k_{\rm e}^{\rm BK}, \eta, \Delta, \gamma_{\rm j} \approx \Phi^{-1}, \theta$ and considering a source at the luminosity distance D_{19} in Gpc with kinetic jet power L_{44} once can calculate the observed power $[\nu S_\nu(\nu > \nu_{\rm b}]_{12}$ in units of 10^{12} Hz Jy

$$[\nu S_\nu]_{12} = 0.03 k_{\rm e} \Delta^{-1} \left(1 + \frac{2}{3} k_{\rm e} \Lambda_{\rm e}\right)^{-1} \gamma_{\rm j}^{-1} D_{\rm j}^3 L_{44} D_{19}^{-2} \qquad (23)$$

While the total proton induced luminosity has the particularly simple form Eq. (16), the cascade spectrum depends on the radiation compactness (shifting E_γ^*) and the magnetic field (shifting the characteristic synchrotron frequency), which can be calculated for a given source at $r_{\rm b}$ from

$$B_{\rm b} = B_1 r_{\rm b,ob}^{-1} \sin\theta$$
$$= k_{\rm e}^{-\frac{1}{6}} \Delta^{\frac{7}{12}} \left(1 + \frac{2}{3} k_{\rm e} \Lambda_{\rm e}\right)^{\frac{7}{12}} \gamma_{\rm j}^{\frac{13}{6}} \beta_{\rm j}^{\frac{19}{12}} D_{\rm j}^{\frac{1}{6}} (\sin\theta)^{\frac{7}{6}} \Phi_{\rm ob} L_{44}^{-\frac{7}{12}} \qquad (24)$$

and Eqs. (18) and (23).

A striking trend follows: $l \propto k_{\rm e}^{\frac{11}{12}} \propto (1+\eta)^{-\frac{11}{12}}$, while $B_{\rm b} \propto k_{\rm e}^{-\frac{1}{6}} \propto (1+\eta)^{\frac{1}{6}}$. But from Eq. (23) one can see that with an increasing proton/electron ratio η the target luminosity (10^{9-16} Hz) decreases, while – because of Eq. (16) – the proton induced luminosity and the magnetic field remain roughly constant. Thus the most luminous gamma ray emitters (relative to their radio to optical luminosity) can emit the highest gamma ray energies in their rest frame (Fig.1).

For very low values of the compactness $l \ll 10^{-6}$, which should not occur in variable sources but in extended hot spots, the spectrum changes radically, since the individual cascade generations show up producing a bumpy spectrum (see MKB). For values $l \gg 10^{-3}$ the X–ray spectral index approaches $\alpha_X = 1$ and the reprocessing becomes partially nonlinear. Such values of l occur when $r_{\rm b}$ is very small, *i.e.* for $r_{\rm b} \ll 1$ pc. It must be emphasized that thermal reprocessing (Zdziarski et al. 1990) is not considered here because of the low thermal gas densities in the jet (cf. Sect. 2.1.1). However, for a compactness value reaching the saturation value the pairs produced by the cascade increase the thermal particle density considerably (leading to a strong annhihilation line). Then the approach of this work is not valid anymore.

There is some heating connected to the relativistic particles. However, particles in the fully ionized jet plasma rather couple to collective degrees of freedom instead of suffering single particle Coulomb interaction. In fact, if the latter process would yield more heat than relativistic particle power, there would not be any acceleration.

It is important to note, however, that while electrons still cool when they are at great distances to the acceleration regions

generating extended emission patterns like radio lobes, protons would not behave in such a way. Their cooling relies on the presence of compact target photon fields.

Fig. 2 shows the variation of θ with η held fixed. It is obvious that in this case the PIC spectrum does not change much its shape, since the compactness is almost constant. However, there is a positive correlation between flux and maximum gamma ray energy (due to Doppler–boosting). The primary electron induced spectrum, the soft spectrum, is interesting in that the break frequency decreases with decreasing flux. Thus observations showing such a correlation would indicate differential Doppler–boosting.

Table 1. Physical parameters inferred for the blazars 3C279 and Mkn421 (H_o = 75 km s^{-1}Mpc^{-1} and q_o = 0.5). Intrinsic parameters as in Fig.1.

	3C279 – High	**– Low**	**Mkn421**
z	0.538	0.538	0.0308
γ_j	20	20	10
θ [deg]	3	5.5	3
η	10	10	1
k_e	0.05	0.05	1
L_{44}	3×10^3	3×10^3	10^{-1}
ν_c [Hz]	10^{14}	10^{14}	10^{16}
ν_b [Hz]	2×10^{11}	7.9×10^{10}	1.6×10^{13}
D_j	19	8.5	15.7
l	2.4×10^{-5}	2.3×10^{-5}	6.5×10^{-4}
B_b[G]	1.4	1.0	90.0
a_s	4.5×10^{-3}	4.5×10^{-3}	5×10^{-1}
$r_{b,ob}$[pc]	5.3×10^{-2}	1.7×10^{-1}	6.7×10^{-6}
$\gamma_{p,b}$	2×10^{11}	2×10^{11}	5×10^9
E^*_γ[TeV]	26.0	13.4	0.8
Φ_{ob} [deg]	38.3	20.1	38.3

2.3. Application

There are no existing data sets covering the enormous bandwidth of the proton blazar spectrum of more than 18 orders of magnitude simultaneously. This makes any interpretatory attempt of data from different epochs difficult, since variability of the blazar emission is present on times scales from days (due to shocks propagating through inhomogenities) to years (due to adiabatic expansion). However, to demonstrate the power of the model Figs.3 and 4 show synthetic spectra approximating observations of the BL Lac object Mkn421 and the OVV quasar 3C279 grouping existing non-simultaneous data into high–state and low–state spectra.

The synthetic spectra do not account for interstellar absorption both in the host galaxy and in the Milky Way. Moreover, the possibly important absorption of gamma rays above 0.1 TeV for sources at redshifts $z \geq 0.1$ on the intergalactic infrared photon background field (Stecker et al. 1992) is not included. This effect would qualify blazars with redshift $z < 0.1$ as the most promising TeV gamma ray candidates, *e.g.* Mkn421 and similar objects like Mkn501, 3C371, Mkn180, IZw186, 4C04.77, PKS0548–322 and PKS0521–365.

The general shape of the PIC spectrum makes it clear that the GRO/EGRET instrument is particularly well–suited to detect proton blazars. The gamma ray spectral index is $\alpha_\gamma \approx 1$ with a tendency for slight hardening and the hard X-ray spectral indices are close to $\langle \alpha_X \rangle \approx 0.5 - 0.7$ consistent with the findings by Worrall & Wilkes (1990). The steepening towards $\alpha_\gamma \approx 1$ occurs in the MeV range, *i.e.* in the GRO/COMPTEL range (cf. Sect. 2.2).

3. Contribution of proton blazars to the diffuse gamma ray and neutrino background

3.1. Diffuse gamma rays

The acceleration of protons should be a generic property of all radio jets. However, as shown above, only the twofold condition of very high proton energies and a (comoving frame) radiation compactness greater than $\approx 10^{-6}$ leads to significant gamma ray fluxes in the extragalactic window $E_\gamma < 100$ TeV. It is assumed here that the conditions are fulfilled at least during blazar episodes in compact radio jets. This assumption is confirmed by the GRO detections. However, further gamma ray measurements must clarify the situation.

Urry et al. (1991) give a present day space density of

$$N_{\rm BL} \approx 4 \times 10^{-8}\,{\rm Mpc}^{-3} \qquad (25a)$$

for BL Lacs at the maximum of the distribution of $N_{\rm BL} L_{\rm r}^2$ at the 2.7 GHz luminosity $L_{\rm r} = 2.7 \times 10^{41}$ erg/s and for flat–spectrum radio quasars correspondingly

$$N_{\rm FSRQ} \approx 3 \times 10^{-10}\,{\rm Mpc}^{-3} \qquad (25b)$$

at $L_{\rm r} = 9 \times 10^{42}$ erg/s. With an average radio/X–ray spectral index $\langle \alpha_{\rm rx} \rangle = 0.82$ one obtains the corresponding X–ray luminosity $L_{\rm X} \simeq 30 L_{\rm r}$. The spectral luminosity of gamma rays from proton blazars is now estimated assuming $\eta = 1$ and $\alpha_\gamma = 1$ (cf. Figs.2,4) yielding $L_E \approx L_{\rm X} E^{-1} \approx 30 L_{\rm r} E^{-1}$.

Relevant for the diffuse flux is the sum of the contributions of both populations BL Lac and FSRQ, each presumably containing a proton blazar. This yields together with a power–law evolutionary scheme

$$\begin{aligned} \langle N_{\rm pb} L_E \rangle &= 30 \left(N_{\rm BL} L_{\rm r} + N_{\rm FSRQ} L_{\rm r} \right) E^{-1} (1+z)^\beta \\ &\approx 4 \times 10^{35}\,{\rm erg\,s^{-1}\,Mpc^{-3}} E^{-1} (1+z)^\beta \end{aligned} \qquad (26)$$

The gamma ray background intensity of the proton blazars for a Friedmann-universe with $q_o = 1/2$ and H_o = 75 km/s /Mpc is then given by

$$I(E) = \frac{3c}{8\pi H_o} \int_0^{z_{\rm max}} N_{\rm pb} L_{E(1+z)} (1+z)^{\beta - 5/2} dz \qquad (27)$$

where z denotes redshift. The result is only weakly dependent on β, *viz.* for $\beta = 3$ and $z_{\rm max} = 1.5$ the intensity has the value

$$I(E) \simeq 2 \times 10^{-8} E_{\rm GeV}^{-1}\,({\rm cm^2\,s\,ster})^{-1} \qquad (28)$$

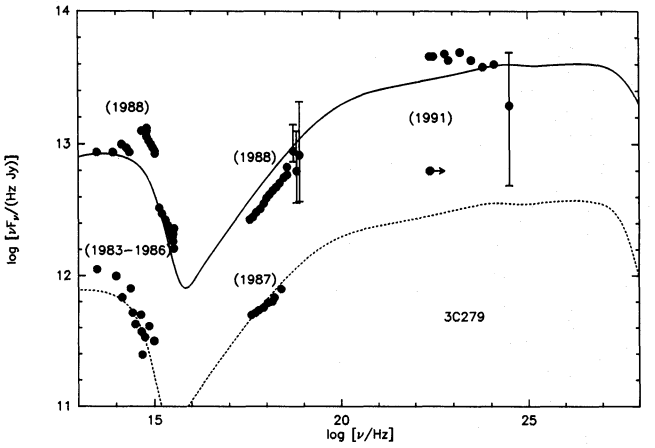

Fig. 3. The OVV quasar 3C279 interpreted as a proton blazar. Data are from the plots in Makino et al. (1989) and Hartman et al. (1992). The synthetic spectrum is produced by shock accelerated electrons below 10^{15} Hz and analogously by accelerated protons above this frequency. The physical conditions leading to the type of spectra shown are listed in Table 1. Note that gamma rays above 0.1 TeV are likely to be absorbed by intergalactic infrared photons.

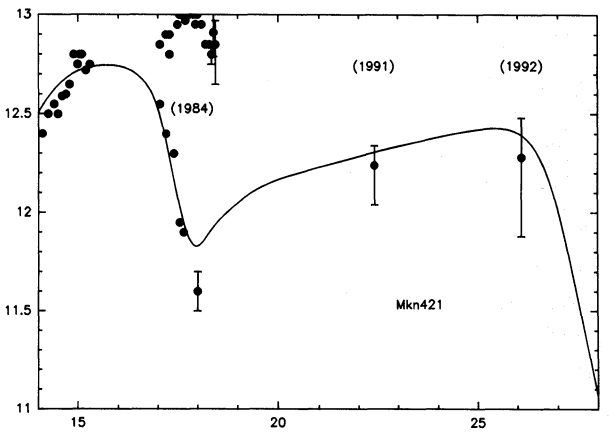

Fig. 4. The Bl Lac object Mkn421. Data are taken from the plots in George et al. (1988), Michelson et al. (1992) and Punch et al. (1992), physical parameters are listed in Table 1. The high–state X–ray emission could still be proton initiated emission, if thermal reprocessing is assumed, *e.g.* caused by a massive screen crossing the compact jet.

This compares to the extrapolated intensity of gamma rays from the Galactic disk

$$I_{\rm G}(E) \simeq 10^{-5} E_{\rm GeV}^{-1.7}\,({\rm cm^2\,s\,ster})^{-1} \tag{29}$$

The two spectra cross each other at $E_\gamma \approx 7$ TeV where the intensity is $I_{7\rm TeV} \simeq 3 \times 10^{-12} ({\rm cm^2\,s\,ster})^{-1}$. The value is well below the quiet uncertain upper limits which can be inferred from measurements reported in Ressell & Turner (1990)

$$I_{20\rm TeV} \leq 10^{-11}\,\left({\rm cm^2\,s\,ster}\right)^{-1} \tag{30}$$

The intergalactic absorption predicted by Stecker et al. (1992) reduces the flux of extragalactic gamma rays above 0.1 TeV to the fluxes of the individual point sources with redshifts $z < 0.1$.

3.2. Diffuse neutrinos

Equation (27) can be used to estimate the flux of neutrinos escaping from the proton blazar (from charged pion decay; kaons and neutrons can be neglected). The neutrino spectrum is very hard $dN/dE \propto E^{-1}$, so that its (comoving frame) luminosity peaks at 1/20 of the proton maximum energy from Eq. (15). This is, of course, in marked contrast to the electromagnetic spectrum where the effect of cascading washes out the memory of the injection energy. The physical reason for the injection at highest energy is that in an inverse power–law target field the highest energy protons find the most target photons (Mannheim & Biermann 1989).

Therefore the observed spectral luminosity not too far from the maximum energy is constant

$$L_{E_\nu} = L_X E_{\nu,\rm max}^{-1} \Lambda_\gamma \tag{31}$$

where $\Lambda_\gamma = \ln E_\gamma^*/E_\gamma^{**} \approx 5$. Normalization guarantees

$$L_\nu = \int L_{E_\nu} dE_\nu = L_X \Lambda_\gamma \approx L_{\rm PIC} \tag{32}$$

(the gamma ray spectral luminosity is lower by the factor Λ_γ^{-1} because of the cascade smearing photons over the energy band from E_γ^* to E_γ^{**}). The omnidirectional flux is then given by

$$F_\nu \approx 10^{-15}\,({\rm cm^2\,s})^{-1} \text{ for } E_\nu < \frac{D_{\rm j} E_{\rm p,max}}{(1+z_{\rm max})20} \approx 10^9\,{\rm GeV} \tag{33}$$

($\gamma_{\rm p,b} \approx 10^{10}$, $D_{\rm j} \approx \langle\gamma_{\rm j}\rangle \approx 7$ from Urry et al. 1991). Equation (33) compares to the flux of atmospheric neutrinos

$$F_\nu(E_\nu) \approx \left[\frac{E_\nu}{\rm GeV}\right]^{-2.3} ({\rm cm^2\,s})^{-1} \tag{34}$$

so that the extragalactic blazar neutrino flux crosses the atmospheric flux at an energy

$$E_\nu^\star \approx 3\,{\rm PeV} \tag{35}$$

where the detection probability of $\bar\nu_{\rm e}$ is enhanced due to the Glashow–Weinberg resonance at 6.4 PeV. The possibility of detecting neutrinos from flat–spectrum radio quasars with the Fly's Eye experiment is investigated in Mannheim et al. (1992). There is a significant chance that the HiRes (Cassiday et al. 1989) might be able to detect proton blazars. Taking into account neutrinos from pp collisions (Sect. 2.1.1) the flux Eq. (33) is changed at low energies to a $F_\nu \propto E^{-1}$ behaviour. Since the $p\gamma$ flux is flat, the de–redshifted energy, at which steepening due to neutrinos from pp collisions occurs, is given by $(1+z_{\rm max})E_{\nu\rm max}7\,[r_{\rm S}/r]$. Assuming an average value of $r \approx 10^3 r_{\rm S}$ (the mean value for 3C279 and Mkn421) one has steepening below $E_\nu \approx 10^7$ GeV. This would decrease the value of E_ν^* to ≈ 1 PeV.

4. Leading neutrons

Hadronic interactions exhibit a unique fingerprint: In every second inelastic proton-photon event the leading nucleon emerging from the interaction fireball is a neutron. Since neutrons are not magnetically confined anymore, they can escape the acceleration region in the jet. The optical depth for neutrons transverse to the jet is less than unity, so that the ultra–relativistic neutrons can leave the source without turning back into confined protons (provided that the distance of the jet from the site of the thermal UV nucleus is great enough to prevent damping by these photons). Since the frame in which the scattering centers isotropize the accelerated protons rests in the bulk flow of the jet, the emitted neutrons as seen from an observer stationary with respect to the host galaxy are streaming along a cone with the blazar in its apex. As a corollary it follows that

Baryonic blazar beams contain energetic photons, neutrinos and neutrons with comparable luminosities.

It remains to be shown, wether the neutrons have observable consequences (cf. Kirk & Mastichiadis 1989).

While it has been suggested by Sikora et al. (1989) and Begelman et al. (1991)[2] that neutrons from a hypothetical accretion disk in an AGN can explain observed gas outflows, the mechanism proposed works best for not too energetic neutrons. To convert the power of the relativistic neutrons into kinetic power of thermal plasma authors assume effective coupling of the two media via excitation of Alfvén–waves by β–decay protons.

However, it is by no means clear how the microphysics shall interplay to lock the particles isotropically to the plasma when their energy is very high (e.g. Berezinskiĭ et al. 1990). It must be remembered that the luminosity of neutrons from the jet peaks at the highest neutron energy ($\approx 10^9$ GeV). Without such isotropic locking there are no adiabatic losses. Moreover, the distance neutrons travel before suffering β-decay is given by

$$R_n = \gamma_n c \Delta\tau_n \approx \left(\frac{\gamma_n}{10^8}\right) \text{ kpc} \tag{36}$$

Proton blazars generating most neutron luminosity at $\gamma_n \geq 10^9$ are therefore clearly injectors of cosmic rays, because the neutrons decay at $R_n \geq 10$ kpc outside the main central galaxy. Only for $\gamma_n < 10^9$ neutrons decay well within the host galaxy. The greatest number of these neutrons come from pp collisions in the jet (Sect. 2.1.1). Their luminosity is much less than that of neutrons from pγ collisions. It must also be remembered that the great luminosity of the proton blazar appears only in the direction of the jet. After isotropization the true luminosity available for conversion into the kinetic power of a wind is reduced by the factor $D_j^{-4} \approx 10^{-4}$.

Nevertheless one can proceed and calculate the expected properties of a neutron driven wind, assuming that after β–decay rapid coupling to the plasma can be achieved. The energy deposition rate for the neutrons is then given by

$$dL_n/dlogE_n \simeq D_j^{-4} L_X \Lambda_\gamma E_n/E_{n,max} \tag{37}$$

due to the hard injection $dN_n/dE_n \propto E_n^{-1}$ (Mannheim & Biermann 1989). Assuming that the neutron luminosity converts into kinetic power at the distance of maximum energy deposition, *i.e.*

$$L_{kin} = \dot{M} c^2 \beta_W^2/2 \simeq D_j^{-4} L_X \Lambda_\gamma \tag{38}$$

yields together with flux conservation (constant mass flux)

$$\rho v_W A = \dot{M} \tag{39}$$

where ρ denotes mass density and A the wind's cross sectional area, the wind speed

$$\beta_W \simeq 10^{-3} \left(\frac{D_j^{-4} L_X \Lambda_\gamma}{5 \times 10^{39}\,\text{erg/s}}\right)^{1/3} \left(\frac{R_{n,max}}{10\,\text{kpc}}\right)^{-2/3} \times \left(\frac{\tan[\Theta]}{\tan[10^o]}\right)^{-2/3} \left(\frac{n_{th}}{10^{-3}\,\text{cm}^{-3}}\right)^{-1/3} \tag{40}$$

and mass flux

$$\dot{M} = 0.2 M_\odot/\text{yr} \left(\frac{D_j^{-4} L_X \Lambda_\gamma}{5 \times 10^{39}\,\text{erg/s}}\right)^{1/3} \left(\frac{R_{n,max}}{10\,\text{kpc}}\right)^{4/3} \times \left(\frac{\tan[\Theta]}{\tan[10^o]}\right)^{2/3} \left(\frac{n_{th}}{10^{-3}\,\text{cm}^{-3}}\right)^{2/3} \tag{41}$$

The opening angle of the cone is denoted as Θ and the value $\Theta \approx 10^o$ is taken from Urry et al. (1991). A motion of the position angle of the compact jet with respect to the large–scale jet may result in an effectively larger cone width. Note that the right hand side of Eq. (38) is a consequence of the cosmic ray energy deposition rate

$$\dot{E}_{cr}(R) = dL_n/dlogE_n(E_n)|_{R=E_n c \Delta\tau_n/m_n c^2} \tag{42}$$

This conical wind surrounding the radio jet in giant radio galaxies would have the remarkable property

$$L_{kin} \propto L_{nth} \propto L_{jet} \tag{43}$$

where L_{nth} denotes the luminosity of the nonthermal blazar. The blazar is, of course, barely observable in FR galaxies where it is beamed in the plane of the sky – unless the contiuum is reradiated by photoionized clouds crossing the beam. On the other hand, when the radio galaxy appears as a blazar, the effect of the wind would be difficult to disentangle, since the blueshifted line (w.r.t. the host galaxy) emitting gas has many orders of magnitude less power.

Equation (43) bears some similiarity with the observational result (Rawlings & Saunders 1990)

$$L_{NLR} \propto L_{jet} \tag{44}$$

[2] cf. MacDonald et al. (1990) for further consequences of energetic neutrino production.

where $L_{\rm NLR}$ denotes the narrow line luminosity. The NLR can be viewed as photoionized clouds reradiating the assumed blazar continuum. However, Eq. (37) shows that because of the high neutron energies most power is deposited many kiloparsecs away from the kinematical center of the galaxy, in contrast to the observed NLR and fast nuclear wind in some FR galaxies, which are found at only a few hundred parsecs. At greater distances from the center extended line emitting structures can still be observed in many FR galaxies (Tadhunter et al. 1989) and the neutron driven wind would imply that these structures represent an outflow.

5. Conclusions

What can be learned from adding relativistic protons to the usual relativistic electrons observed in compact radio jets?

First of all, if the protons manage to be accelerated up to the high energies where their energy loss rate is equal to the electron energy loss rate, they generically induce high energy emission from X–rays to gamma rays. The flux spectrum of the polarized synchrotron cascade radiation has an index $0.5 - 0.7$ at X–ray frequencies steepening in the MeV range to a gamma ray flux with index $0.8 - 1.0$ up to the TeV range. The electromagnetic synchrotron showers in the jet are unsaturated (only four generations of photons) and yield neither a significant annihilation line nor much thermal energy.

At present it is unknown, wether there is also a generic proton/electron ratio η and hence a generic ratio $L(> X)/L(< UV)$. The EGRET detections of flat–spectrum sources seem to indicate that either there is significant scatter in the distribution of η or that the proton acceleration (taking longer than the electron acceleration) is sometimes interrupted before reaching the maximum proton energies. Proton enrichment $\eta > 1$ increases the ratio of gamma rays to radio photons, so that it is clear, why EGRET found radio sources below the 1 Jy level with stronger gamma ray emission than sources with radio fluxes above 1 Jy.

Secondly, with protons brought into the game, the flat–spectrum radio sources generate a diffuse background of gamma rays and neutrinos both of which are detectable with planned experiments above 7 TeV and 1 PeV, respectively.

Finally, the presence of protons leads to neutron production which has remarkable astrophysical consequences. At ultra–high energies the neutrons escape from the host galaxy without adiabatic losses injecting cosmic ray protons. At lower energies they can accelerate gas surrounding the radio jet within the host galaxy (and its halo).

Acknowledgements. I acknowledge support by DARA grant FKZ 50 OR 9202 and many helpful discussions with P.L. Biermann. A. Witzel and R. Wegner from the VLBI–group in Bonn have contributed with their experience and expertise about the fascinating realm of superluminal radio sources. I also acknowledge discussions with R. Schlickeiser about the issue of leptonic vs. baryonic cosmic rays and helpful comments on the manuscript by A. Zdziarski.

References

Begelman, M.C., de Kool, M., Sikora, M., 1991, *Astrophys. J.*, **382**, 416
Bell, A.R., 1978, *Monthly Notices Roy. Astron. Soc.* **182**, 443
Berezinskiĭ, V.S., Bulanov, S.V., Dogiel, V.A., Ginzburg, V.L. (ed.), Ptuskin, V.S., 1990, *Astrophysics of Cosmic Rays*, North Holland, Amsterdam
Biermann, P.L., Strittmatter, P.A., 1987, *Astrophys. J.*, **322**, 643
Biermann, P.L., 1991, in: *Frontiers in Astrophysics,* eds. R. Silberberg, G. Fazio, M. Rees, Cambridge
Blandford, R.D., Königl, A., 1979, *Astrophys. J.*, **232**, 34
Bregman, J.N., 1990, *Astron. Astrophys. Rev.*, **2**, 125
Burns, M.L., Lovelace, R.V.E., 1982, *Astrophys. J.*, **262**, 87
Cassiday, G.L., et al., 1989, in: *Proc. of the Workshop on Particle Astrophysics: Forefront Experimental Issues, held at the University of California, Berkley, Dec 8-10*, ed. E.B. Norman, World Scientific, Singapore, p. 259
Ellison, D.C., Jones, F.C., Reynolds, S.P., 1990, *Astrophys. J.*, **360**, 702
Fanaroff, B.L., Riley, J.M., 1984, *Monthly Notices Roy. Astron. Soc.* **167**, 31P
George, I.M., Warwick, R.S., Bromage, G.E., 1988, *Monthly Notices Roy. Astron. Soc.* **232**, 793
Giovanoni, P.M., Kazanas, D., 1990, *Nature*, **345**, 319
Halzen, F., Zas, E., 1992, *University of Wisconsin – Madison*, Preprint MAD/PH/695
Hartman, R.C., et al., 1992, *Astrophys. J.*, **385**, L1
Kellermann, K.I., Pauliny-Toth, I.K., 1969, *Asrophys. J.*, **155**, L71
Kirk, J.G., Mastichiadis, A., 1989, *Astron. Astrophys.*, **211**, 75
Königl, A., 1981, *Astrophys. J.*, **243**, 700
MacDonald, J., Stanev, T., Biermann, P.L., 1991, *Astrophys. J.*, **378**, 30
Makino et al., 1989, *Astrophys. J.*, **347**, L9
Mannheim, K., Biermann, P.L., 1989, *Astron. Astrophys.*, **221**, 211
Mannheim, K., Krülls, W.M., Biermann, P.L., 1991, *Astron. Astrophys.*, **251**, 723
Mannheim, K., Biermann, P.L., 1992, *Astron. Astrophys.*, **253**, L21
Mannheim, K., Stanev, T., Biermann, P.L., 1992, *Astron. Astrophys.*, L1
Maraschi, L., Maccacaro, T. Ulrich, M.-H. (eds.), 1989, *Proc. of the Workshop on BL Lac Objects*, Lecture Notes in Physics, Vol. 334, Springer Verlag, Berlin, Heidelberg, New York
Michelson et al., 1992, *IAU Circ.* No. 5470
Protheroe, R.J., Szabo, A.P., 1992, *submitted to Nature*
Punch, C.W. et al., 1992, *Nature*, **358**, 477
Qian, S.J., Quirrenbach, A., Witzel, A., Krichbaum, T.P., Hummel, C.A., Zensus, J.A., 1991, *Astron. Astrophys.*, **241**, 15
Quirrenbach, A., Witzel, A., Wagner, S., Sanchez–Pons, F., Krichbaum, T.P., Wegner, R., Anton, K., Erlens, U., Hähnelt, M., Zensus, J.A., Johnston, K.J., 1991, *Astrophys. J.*, **372**, L71
Rachen, J.P., Biermann, P.L., 1992, *to be submitted to Astron. Astrophys.*
Rawlings, S., Saunders, R., 1991, *Nature*, **349**, 138
Ressell, M.T., Turner, M.S., 1990, *Comments Astrophys.*, Vol. 14, No. 6, 323
Sikora, M., Kirk, J.G., Begelman, M.C., Schneider, P., 1987, *Astrophys. J.*, **320**, L81
Sikora, M., Begelman, M.C., Rudak, B., 1989, *Astrophys. J.*, **341**, L33
Stecker, F.W., De Jager, O.C., Salamon, M.H., 1992, *Astrophys. J.*, **390**, L49

Stenger, V.J. et al. (eds.), 1992, *High Energy Neutrino Astrophysics*, Proc. of the Workshop held at the Univ. of Hawaii at Manoa, Honolulu, Hawaii 23–26 March 1992, World Scientific, Singapore, in press

Svensson, R., 1987, *Monthly Notices Roy. Astron. Soc.*, **227**, 403

Tadhunter, C.N., Fosbury, R.A.E., di Serego Aligheri, S., 1989 in: *Proc. of the Workshop on BL Lac Objects*, Lecture Notes in Physics, Vol. 334, eds. L. Maraschi, T. Maccacaro and M.-H. Ulrich, Springer Verlag, Berlin, Heidelberg, New York, p. 79

Urry, C.M., Shafer, 1984, *Astrophys. J.*, **280**, 569

Urry, C.M., Padovani, P., Stickel, M., 1991, *Astrophys. J.*, **382**, 501

Witzel, A., 1990, in: *Parsec–Scale Radio Jets*, eds. J.A. Zensus, T.J. Pearson, Cambridge University Press, p. 206

Worrall, D.M., Wilkes, B.J., 1990, *Astrophys. J.*, **360**, 396

Zdziarski, A.A., Ghisellini, G., George, I.M., Svensson, R., Fabian, A.C., Done, C., 1990, *Astrophys. J.*, **363**, L1

Zensus, J.A., Pearson, T.J. (eds.), 1987, *Proc. of a Workshop on Superluminal Radio Sources, held at Big Bear Solar Observatory, California, Oct 28-30, 1986*, Cambridge University Press